N.P. KLOCHKO,[1] V.R. KOPACH,[1] S.I. PETRUSHENKO,[2,3] E.M. SHEPOTKO,[1]
S.V. DUKAROV,[2] V.M. SUKHOV,[2] A.L. KHRYPUNOVA[1]

[1] National Technical University "Kharkiv Polytechnic Institute"
(2, Kirpichov Str., Kharkiv 61002, Ukraine)
[2] V.N. Karazin Kharkiv National University
(4, Svobody Square, Kharkiv 61022, Ukraine)
[3] Technical University of Liberec, Institute for Nanomaterials,
Advanced Technologies and Innovation, Department of Advanced Materials
(460 01 Liberec, Czech Republic; e-mail: petrushenko@karazin.ua)

UDC 538.975; 53.096

COPPER-ENRICHED NANOSTRUCTURED CONDUCTIVE THERMOELECTRIC COPPER(I) IODIDE FILMS OBTAINED BY CHEMICAL SOLUTION DEPOSITION ON FLEXIBLE SUBSTRATES

The objects of our research are flexible thin-film thermoelectric materials with nanostructured CuI layers 0.5–1.0 μm thick, fabricated by the chemical solution method Successive Ionic Layer Adsorption and Reaction (SILAR) on flexible polyethylene terephthalate and polyimide substrates. These cubic γ-CuI films differ from films obtained by other chemical solution methods, such as spin-coating, sputtering, and inject printing, in their low resistivity due to acceptor impurities of sulfur and oxygen introduced into CuI from aqueous precursor solutions during SILAR deposition. Energy barriers at the boundaries of 18–22 nm CuI nanograins and a large number of charge carriers inside the nanograins determine the transport properties in the temperature interval 295–340 K characterized by transitions from semiconductor to metallic behavior with increasing temperature, which are typical of nanostructured degenerate semiconductors. Due to the resistivity of about 0.8 m$\Omega\cdot$m at 310 K and the Seebeck coefficient 101 μV/K, the thermoelectric power factor of the CuI film 1.0 μm thick on the polyimide substrate is 12.3 μW/(m$\cdot$K^2), which corresponds to modern thin-film p-type thermoelectric materials. It confirms the suitability of CuI films obtained by the SILAR method for the fabrication of promising inexpensive non-toxic flexible thermoelectric materials.

Keywords: copper(I) iodide, thermoelectricity, carrier transport, nanostructure, thin film, chemical solution process.

1. Introduction

Copper(I) iodide (CuI) is a promising semiconductor with band gap E_g equal to 3.1 eV, which has been widely used in heterojunction diodes, thermoelectric (TE) devices, photodetectors, solar cells and transistors [1–7]. By an appropriate doping, CuI provides high hole mobility up to 44 cm^2 V^{-1}s^{-1}, and p-type conductivity up to 280 S$\cdot$cm^{-1} with a wide range of hole concentrations (from 10^{16} to 10^{20} cm^{-3}) [5]. The excellent electrical characteristics of CuI are due, firstly, to the electronegativity of iodine of 2.66

Citation: Klochko N.P., Kopach V.R., Petrushenko S.I., Shepotko E.M., Dukarov S.V., Sukhov V.M., Khrypunova A.L. Copper-enriched nanostructured conductive thermoelectric copper(I) iodide films obtained by chemical solution deposition on flexible substrates. *Ukr. J. Phys.* **69**, No. 2, 115 (2024). https://doi.org/10.15407/ujpe69.2.115.
Цитування: Клочко Н.П., Копач В.Р., Петрушенко С.І., Шепотько Є.М., Дукаров С.В., Сухов В.М., Хрипунова А.Л. Збагачені міддю наноструктуровані провідні термоелектричні плівки йодиду міді(I), отримані на гнучких підкладинках методом хімічного осадження з розчину. *Укр. фіз. журн.* **69**, №2, 115 (2024).

on the Pauling scale, which allows the appearance of many delocalized holes above the valence band maximum [5]. Secondly, the large I^- radius of 220 pm and the spatially spread three outermost p-orbitals can achieve sufficient orbital overlap for the fast hole transport [5]. An advantageous feature is that CuI consists of abundant non-toxic elements.

The copper(I) iodine films with stable cubic structure γ-CuI can be grown by a variety of physical vapor and chemical solution methods at near room temperatures [2, 5, 7]. To date, the best thermoelectric figures of merit (ZT) have been obtained for CuI films prepared by the solid iodination of copper layers on glass substrates ($ZT \approx 0.22$) [7], an,d for CuI films deposited on a flexible polyethylene, terephthalate (PET) substrates by reactive sputtering ($ZT \approx 0.21$) [2]. The above has accelerated the realization of the flexible thermoelectric devices for body-heat-driven wearable electronics, as well as for on-chip cooling or power reversion of miniaturized chips [5].

At the same time, the continuous pursuit of cost-effective manufacturing is increasingly redirecting the research efforts to the chemical solution-based coating approaches, because they do not require expensive high-vacuum processing chambers. Additionally, the chemical solution deposition processes has other advantages, such as large area atmospheric deposition capabilities, easy operation, and component adjustment [5, 6]. But till now, CuI thin films synthesized by chemical solution processes such as spin-coating, spraying, ink-jet printing, and vacuum-assisted filtration of a CuI suspension, contain unwanted impurities from the precursor solutions, have insufficient electrical conductivity σ [2, 5, 8], and, as a result, their thermoelectric power factor $P = \sigma S^2$ is small or even negligible (here, S is the Seebeck coefficient). Moreover, CuI thin films obtained by spin-coating, spraying and ink-jet printing require annealing after growth. This creates obstacles for their semiconductor applications, especially for flexible electronics and thermoelectrics [5]. In contrast, the chemical solution deposition process Successive Ionic Layer Adsorption and Reaction (SILAR) does not require annealing after deposition [6, 9, 10], which makes it possible to obtain conductive thermoelectric copper(I) iodide films on various rigid plates or flexible plastic substrates.

According to the data of the authors who obtained effective thermoelectric CuI films by ion-beam sputtering [1], solid-phase iodination [3], and gas-phase iodination [4] of sputtered Cu metal films, iodine-enriched CuI films have higher electrical conductivity and better thermoelectric properties, since they contain many native copper vacancy (V_{Cu}) defects. The V_{Cu}) has a lower formation energy than other intrinsic defects such as I vacancy (V_I), Cu interstitial (Cu_i), I interstitial (I_i), Cu antisite (Cu_I), and I antisite (I_{Cu}) [1, 11]. However, due to the inherent volatility of iodine, the surface layers of iodine-enriched CuI films are unstable, especially under operating conditions at elevated temperatures in thermoelectric devices [1, 3, 4]. In the copper-rich surface regions of CuI films, the iodine V_I vacancy acts as an electron donor; in addition, the deficiency of I suppresses the formation of V_{Cu}, reducing the hole density, so that both of the above factors reduce the conductivity of CuI [1]. Therefore, these CuI films require additional post-growth processing. For example, in [1], the vacuum annealing was used to stabilize films obtained by ion-beam sputtering. In [3], thin CuI films obtained by solid-phase Cu iodination were annealed in argon at 300 °C and then in synthetic air at 150 °C. In addition, the authors of [3, 4, 5] found that iodine vacancies, which are easily formed during the CuI film deposition and annealing in the above physical processes, can be passivated by controlled incorporation of acceptor impurities such as group VI elements O and S. The chalcogen elements O and S are acceptors [3, 5, 11], and one hole could be released after replacing lattice iodine in CuI. According to [5], the substitution of iodine by these p-type dopants under copper-rich conditions seems to be a promising approach that can not only improve thermal stability, but also increase the hole concentration.

The advantage of chemical solution deposition is the easy introduction of foreign atoms, which is convenient and efficient for doping [5]. In our earlier works [9, 10], we found that CuI films obtained by the SILAR method on various substrates are enriched in copper, but contain sulfur and possible oxygen, which enter them from aqueous precursor solutions. The aim of this work is to study the morphology, chemical composition, crystal structure, and charge transport in nanostructured conducting thermoelectric copper(I) iodide films obtained by the SILAR method to create flexible thermoelectric materials. Since the choice of substrate material in the manufacture of thin-film thermoelectric devices plays an important

role in their output thermoelectric parameters [2], herein, for CuI deposition by the SILAR method, we used two polymer substrates important for application in flexible devices: polyethylene terephthalate and polyimide (PI) (Kapton®type). Thus, the objects of our research are flexible thin-film CuI/PET and CuI/PI samples with nanostructured CuI layers fabricated by the SILAR method.

2. Experimental

To create CuI/PI and CuI/PET samples, we used flexible 25 μm thick polyimide (PI, Kapton-HN®) and 20 μm thick polyethylene terephthalate (PET, Toray Industries, Inc.) substrates. Two pieces of PI and PET 2×3 cm in size were tightly inserted into one frame, so that CuI films were deposited from aqueous solutions by the SILAR method only on one side of each substrate. All chemicals used were of high purity and supplied from Sigma Aldrich, Germany. Solutions were prepared from purchased reagents without additional purification and used at room temperature. According to [12], in a solution of a cationic precursor containing 0.1 M $CuSO_4$ and 0.1 M $Na_2S_2O_3$, a complex of copper(I) thiosulfate $[Cu(S_2O_3)]^-$ was formed. The substrates were immersed in this cationic precursor for 20 s. Then the substrates were washed with distilled water for 10 s. After that, they were immersed for 20 s in a 0.05 M NaI solution (anionic precursor) to carry out the reaction of Cu^+ ions strongly adsorbed on the surfaces of PI and PET with I^- ions to obtain CuI. The final stage of one SILAR cycle was rinsing in the distilled water for 10 s. Such SILAR cycles for CuI deposition were repeated 40 or 80 times. The thickness of the CuI films in the CuI/PI and CuI/PET samples thus obtained, estimated according to [1] gravimetrically using a material density of 5.67 g/cm^3, was in the interval of 0.5–1.0 μm.

The surface morphology of CuI/PI and CuI/PET thermoelectric materials was observed using scanning electron microscopy (SEM) in the secondary electron mode without the use of additional conductive coatings. The SEM Tescan Vega 3 LMH operated at an accelerating voltage of 30 kV. Chemical analysis of thermoelectric materials was carried out by X-ray fluorescence (XRF) microanalysis using a Bruker XFlash 5010 with energy dispersive X-ray spectrometry (EDS) system. The energy dispersion spectra were taken from areas 50×50 μm in size. The quantitative evaluation of the spectra was carried out in the mode of a self-calibrating detector.

X-ray diffraction analysis (XRD) of CuI films in CuI/PI and CuI/PET samples was performed on a Shimadzu XRD-6100 diffractometer with monochromatized CuK_α radiation ($\lambda = 1.54060$ Å) operating in the Bragg–Brentano (θ–2θ) geometry. Crystalline phases were identified by comparing the experimental diffraction patterns with the JCPDS reference database using PCPDFWIN v.1.30 software. The average crystallite size D (more precisely, the size of coherent scattering regions in the direction normal to the reflecting plane) in the CuI film was estimated by X-ray line broadening using the Scherer formula [13]:

$$D = (0.9\,\lambda)/(\beta\cos\theta), \qquad (1)$$

where 0.9 is the Scherer constant; $\beta = B - b$ (B is observed Full Width at Half Maximum (FWHM), and b is broadening in the peak due to the instrument) in radians; θ denotes the Bragg angle for the X-ray diffraction peak γ-CuI (111).

Microstrains in the crystal lattice were obtained from the relation $\varepsilon = \Delta d/d$ (where d is the interplanar spacing of the crystal according to JCPDS, and Δd is the difference between the corresponding experimental and reference interplanar spacins). The dislocation density was estimated in accordance with [14] as $1/D^2$.

Resistivity $\rho = \sigma^{-1}$ of CuI films in CuI/PI and CuI/PET samples was measured at near-room temperatures in the interval T 295–340 K in accordance with [15] using a four-point collinear probe resistivity method. The resistivity was calculated as follows:

$$\rho = (\pi\, t\, \delta\, U_{23})\,/\,(I_{14}\ln(2)), \qquad (2)$$

where U_{23} is the voltage between the second and third probes; I_{14} is the current between the first and fourth probes; δ is a correction factor for the accounting the ratio of the distance between the probes and the size of the substrate; $\pi\delta/\ln(2) \approx 4.45$.

To evaluate the thermoelectric characteristics of the obtained CuI/PI and CuI/PET samples at near-room temperatures, the in-plane Seebeck coefficients S were measured as thermoelectric voltages U induced in response to temperature gradients ΔT between hot and cold gold probes on the CuI surfaces

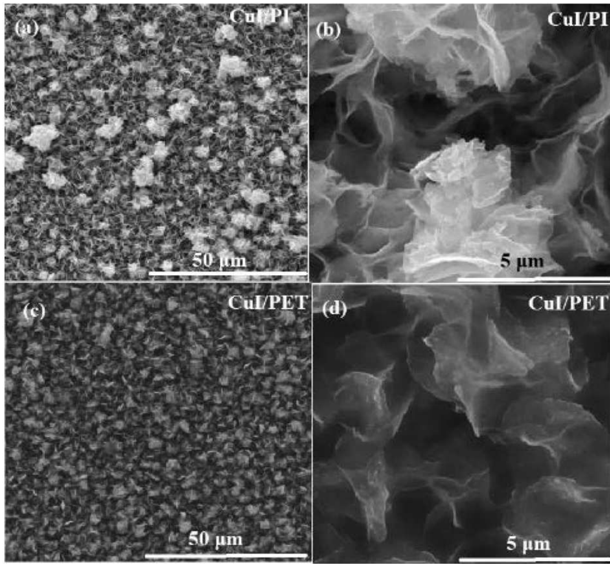

Fig. 1. SEM images at two different magnifications of CuI films deposited by the SILAR method on flexible PI and PET substrates: CuI/PI sample with CuI thickness $t = 1.0$ μm (*a*), (*b*); CuI/PET sample with CuI thickness $t = 0.9$ μm (*c*), (*d*)

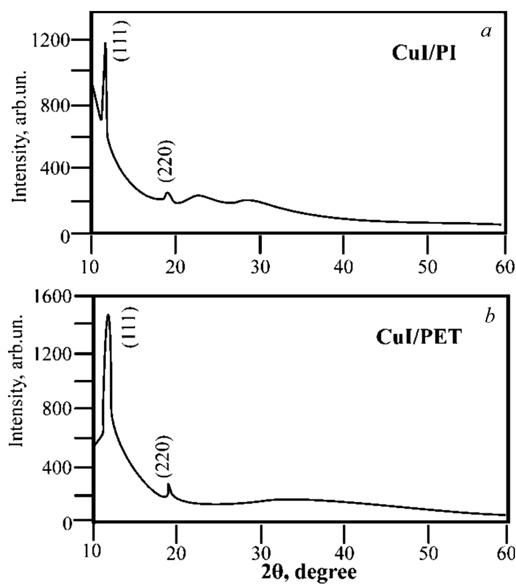

Fig. 2. XRD patterns of CuI/PI sample with CuI film 1.0 μm thick (*a*) and of CuI/PET sample with CuI film 0.9 μm thick (*b*), which were deposited by the SILAR method

in the temperature interval of 295–340 K. The thermoelectric power factors P for flexible CuI/PI and CuI/PET materials were calculated from the above data as S^2/ρ at 310 K.

3. Results and Discussion

Figure 1 shows the morphologies of CuI films prepared on PI and on PET substrates by the SILAR method. SEM images at low magnification in Fig. 1, *a* and *c* show that the CuI films in both samples are not smooth, but do not contain pores and completely cover the surfaces of hydrophobic PI and PET plastic substrates. Petal-like intertwining submicron-thickness nanosheets are seen on the surface of both SILAR-deposited CuI films in the SEM images at high magnification in Figs. 1, *b* and *d*.

The nanoscale structure of these films is confirmed by the X-ray diffraction patterns shown in Figs. 2. It is observed that both CuI films have a structure of the cubic zinc blende type (γ-CuI, JCPDS #06-0246), and the film growth is oriented in the (111) direction. According to the Scherer formula (1), the average crystal size of CuI D is 22 nm in the CuI/PI sample and 18 nm in the CuI/PET sample. Analysis of the structural parameters of CuI revealed tensile microstrains $\varepsilon \approx 6\times10^{-3}$ in CuI/PI and $\varepsilon \approx 8\times10^{-3}$ in CuI/PET. The dislocation density in CuI is in the range (2–4) $\times10^{15}$ lines/m^2.

Chemical X-ray fluorescence microanalysis of these CuI/PI and CuI/PET samples in Fig. 3 and the data of their energy dispersive X-ray spectrometry in Table. 1 show that both CuI films are enriched in copper. The Cu/I atomic ratio is 1.17 in the CuI/PI sample and 1.15 in the CuI/PET sample. Some peaks of the other elements have also been found in the XRF spectra, among which a small peak of aluminum is apparently generated by aluminum attachments of the vacuum chamber, in which the XRF microanalysis was carried out, mainly a table and a sample holder. Oxygen and carbon in the XRF spectra can be attributed to H_2O, O_2, and CO_2 adsorbed on the surface of CuI films. Moreover, O and C are the main elements of PI and PET organic polymeric substrates. Taking into account the small thicknesses of the CuI films, the components of the substrates can quite well be detected by XRF and EDS methods. In addition, since the films were obtained as a result of chemical transformations in aqueous solutions, including those involving an oxygen-containing cationic precursor with the $[Cu(S_2O_3)]^-$ complex, it is quite possible that oxygen can be included in the CuI crystal lattice. The authors of [3, 5, 11] consider such mechanisms related to doping with oxygen as

the passivation of defects due to the elimination of donor levels in CuI or the replacement of iodine (and iodine vacancies, taking into account the Cu/I ratio) by oxygen, which increase p-type doping and, as a result, enhance the conductivity of CuI. It is important that XRF spectra of CuI/PI and CuI/PET samples contain quite a lot of sulfur atoms. The presence of sulfur is a distinctive feature of CuI films obtained by the SILAR method [9, 10], since the solution of the cationic precursor contains a chemically unstable thiosulfate ion. According to [4, 5], the acceptor impurity S can replace iodine and iodine vacancies and thereby increase the conductivity of CuI. Thus, the SILAR method ensures doping of CuI films with sulfur and, presumably, with oxygen, which provides them with electrical conductivity, despite the nanoscale morphology and nano-sized crystals.

The p-type conductivity of the CuI films obtained by the SILAR method is confirmed by the plots of thermoelectric voltages U induced in response to temperature gradients ΔT along the CuI/PI and CuI/PET samples in Fig. 4. The values of the Seebeck coefficient, calculated as $S = U/\Delta T$, are about 100 μV/K at the CuI film thickness of 1.0 μm in the CuI/PI sample and the CuI film thickness of 0.9 μm in the CuI/PET sample (Table 1). Lower thermoelectric voltages for CuI/PI and CuI/PET samples with thinner CuI films in Fig. 4 are explained, according to [16], by parasitic heat flows into the substrates. As can be seen from Fig. 4, the S values are constant in the temperature interval 295–340 K.

As can be seen in Fig. 5, the CuI films deposited by the SILAR method have low resistivity. Their values of ρ are the same as in the ion-beam deposited and vacuum-annealed CuI films in [1], as well as in CuI films obtained in [3] by the solid iodination method from a thin-film copper precursor and stabilized by annealing in argon and in synthetic air. Moreover, CuI films deposited in this work are approximately 100 times more electrically conductive than CuI films obtained by the gas-phase iodination of Cu films in [4], and many other thermoelectric CuI films deposited by various physical vapor methods [5]. Meanwhile, in Fig. 5, the CuI/PI samples show lower resistivity than the CuI/PET samples, which, according to XRD data, can be explained by larger crystal grains of the CuI film on the PI substrate. Graphs of resistivity versus temperature in Fig. 5, *a, d* show transitions from semiconductor to metallic behavior with increasing the temperature with typical ρ minima in all samples. Similar crossovers were observed in [17, 18] for CuI nanocrystalline thin films, which were deposited by physical vapor and chemical solution methods. Semiconductor properties are more pronounced in CuI/PET samples in the interval from room temperature to 310 K (Fig. 5, *d*). The branches of the resistivity vs. temperature graphs with $d\rho/dT < 0$ are explained, according to [17], by the nanoscale structure of CuI films. According to [13, 17, 18], a model capable of reproducing the semiconductor behavior of CuI thin films is the fluctuation-induced tunneling conductivity (FITC) model devel-

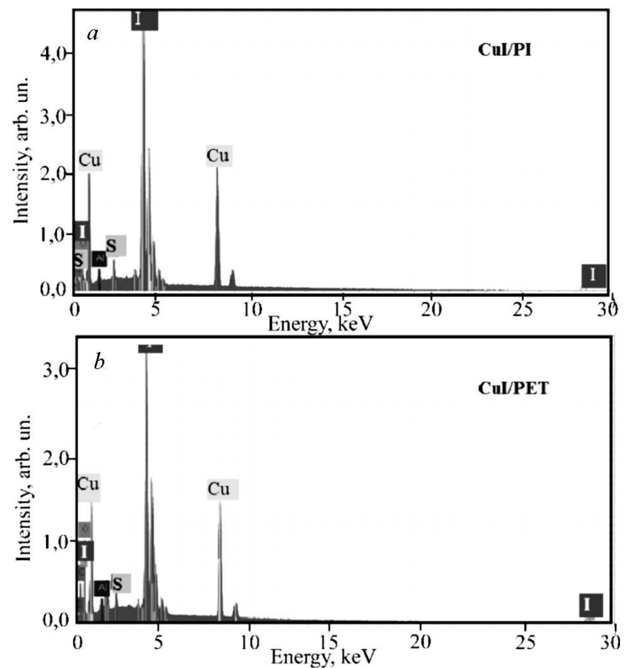

Fig. 3. XRF spectra of CuI/PI sample with CuI film 1.0 μm thick (*a*) and of CuI/PET sample with CuI film 0.9 μm thick (*b*), which were deposited by the SILAR method

Table 1. **Chemical composition and the Seebeck coefficients of CuI/PI and CuI/PET samples**

Sample	Chemical composition, at. %						S, μV/K
	Cu	I	S	O	C	Al	
CuI/PI	34	29	3	8	23	3	101
CuI/PET	15	13	1	23	47	1	102

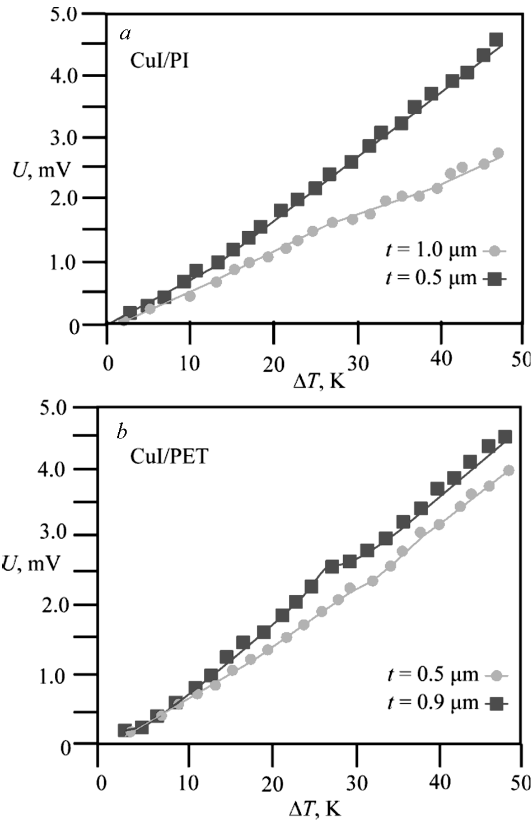

Fig. 4. Thermoelectric voltages induced in response to temperature gradients ΔT along thermoelectric materials CuI/PI (a) and CuI/PET (b) with CuI films of different thicknesses t deposited by the SILAR method

Table 2. **Transport properties and thermoelectric power factors of CuI/PI and CuI/PET samples with CuI films deposited by the SILAR method**

Sampl	t, μm	T_0, eV	ρ_{02}, m$\Omega\cdot$m/K^2	P, μW/(m$\cdot$K^2)
CuI/PI	0.5	86	0.14	2.3
CuI/PI	1.0	22	0.07	12.3
CuI/PET	0.5	123	0.13	4.2
CuI/PET	0.9	72	0.14	5.3

oped by Sheng [19] for a close approach region between two conductive segments separated by an insulating barrier in a disordered material. According to the FITC model, due to the chaotic thermal motion of electrons in the conductive segments, there may be a temporary excess or deficiency of charges on the surfaces of the tunnel junction, which leads to voltage fluctuations at the junction that changes the probability of electron tunneling. As was shown in [13, 17, 18], the FITC model is applicable to degenerate thin CuI films, when most conduction electrons are delocalized and free to move over several atomic distances inside crystal grains. Along with this, the FITC model assumes the presence of energy barriers in nanostructured CuI films at the grain boundaries between the conductive regions of the grains, which are overcome by the tunneling process. As a special case of FITC [17, 18], it was proved in [13] that the transport of charge carriers in polycrystalline CuI films occurs through localized states, along the nearest neighbors, when holes jump over the nearest neighboring empty sites. The temperature dependence of the resistivity according to the mechanism is the nearest neighboring hopping, when $\mathrm{d}\rho/\mathrm{d}T < 0$, has the following form [13]:

$$\rho(T)\ \exp(T_0/T), \tag{3}$$

where T_0 is a characteristic temperature (i.e., T_0 is the hopping energy in Kelvin degree). Thus, for the branch of the resistivity vs. temperature graph, where $\mathrm{d}\rho/\mathrm{d}T < 0$, the slope of the linear fitting of $\ln(\rho)$ vs $1/T$ gives the hopping energy T_0, which is lesser than the activation energy required for the thermally activated transition of charge carriers to the valence band. The hopping energy values calculated from the graphs in Fig. 5, *b, e* are given in Table 2. It can be seen that the energy barriers for transport of charge carriers by the nearest neighboring hopping are higher in thin and fine-grained films, for example, in the CuI/PET sample with CuI thickness of 0.5 μm, which is consistent with its higher resistivity. The thicker CuI film in the CuI/PI sample has the T_0 value of only 22 mV, i.e., the dependence of its conductivity on the temperature is typical of degenerate semiconductors.

In accordance with [17, 18], the modeling of the transport properties, when CuI films in the CuI/PI and CuI/PET samples demonstrate a metallic behavior (for the branch of the resistivity vs. temperature graph, where $\mathrm{d}\rho/\mathrm{d}T > 0$) leads to an insight into the properties of the interior of the CuI grains. As described in [20], when the concentration of charge carriers, including the concentration of ionized impurities, exceeds the critical concentration of carriers, the enhancement of the Coulomb interaction leads to

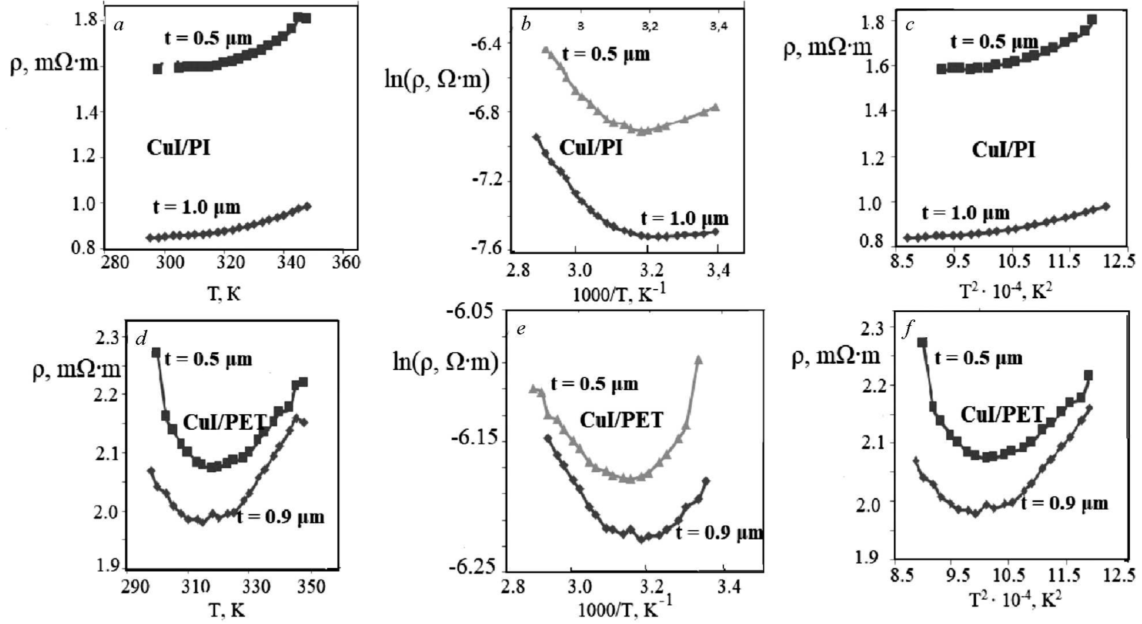

Fig. 5. Temperature dependences of resistivity ρ for thermoelectric materials CuI/PI (*a*, *b*, *c*) and CuI/PET (*d*, *e*, *f*) with CuI films of thickness t: graphs of resistivity versus temperature T (*a*, *d*); graphs $\ln(\rho)$ versus $1000/T$ (*b*, *e*); graphs of ρ versus T^2 (*c*, *f*)

a decrease in the mobility and, consequently, an increase in the resistivity with the temperature, which is typical of metallic behavior. As can be seen from Fig. 5, *c*, *f*, at T above 310 K, when $\mathrm{d}\rho/\mathrm{d}T > 0$, the resistivity of all CuI films deposited by the SILAR method obeys a power law, $\rho(T) \sim T^2$, according to the model of carrier-carrier scattering and scattering by ionized impurities for degenerate semiconductors [17, 18, 20]:

$$\rho(T) = \rho_0 + \rho_{02}T^2, \tag{4}$$

where ρ_0 is a residual offset resistivity at $T = 0$ K, ρ_{02} is a temperature-independent prefactor. The low value of ρ_{02} for the CuI/PI sample with CuI thickness of 1.0 μm in Table 2 shows that its resistivity weakly depends on the temperature, which, according to [20], indicates a high concentration of holes. Thus, the reason for the lower resistivity of this sample is the larger nanocrystals having more free charges and the low energy for the charge tunneling through the grain boundaries.

The values of the thermoelectric power factors in Table 2 confirm the suitability of copper(I) iodide films produced by the SILAR method for the manufacture of an inexpensive non-toxic flexible thermoelectric material. These P data are similar to those presented in [3, 21, 22] for numerous p-type thin-film materials obtained using various techniques, including CuI thin films obtained by the solid-phase Cu iodination annealed in argon and then in synthetic air.

4. Conclusions

Films of copper(I) iodide with a thickness of 0.5–1.0 μm and a crystal grain size of 18–22 nm were deposited by the SILAR method on flexible polyethylene terephthalate and polyimide substrates. These films with a cubic structure of γ-CuI differ from films obtained by other chemical solution methods by low resistivity due to acceptor impurities of sulfur and oxygen, which enter them from precursor solutions during the deposition by the SILAR method. Energy barriers at the boundaries of CuI nanograins and a large number of charge carriers inside the nanograins determine the transport properties at near room temperatures, with transitions from semiconductor to metallic behavior with increasing the temperature, which is typical of nanostructured degenerate semiconductors. Due to the resistivity of about 0.8 $\mathrm{m\Omega \cdot m}$ at 310 K and the Seebeck coefficient

S = 101 μV/K, the thermoelectric power factor of the CuI film 1.0 μm thick on the polyimide substrate is 12.3 μW/(m $\cdot$ K^2). This corresponds to modern p-type thin-film thermoelectric materials and confirms the suitability of CuI films obtained by the SILAR method for the manufacture of promising inexpensive non-toxic flexible thermoelectric materials.

The work was supported by the Ministry of Education and Science of Ukraine and within the MSCA4Ukraine project funded by the European Union.

1. P.P. Murmu, V. Karthik, S.V. Chong, S. Rubanov, Z. Liu, T. Mori, J. Yi, J. Kennedy. Effect of native defects on thermoelectric properties of copper iodide films. *Emergent Mater.* **4**, 761 (2021).
2. A.S. Lemine, J. Bhadra, N.J. Al-Thani, Z. Ahmad. Promising transparent and flexible thermoelectric modules based on p-type CuI thin films – a review. *Energy Reports* **8**, 11607 (2022).
3. P. Darnige, Y. Thimont, L. Presmanes, A. Barnabé. Insights into stability, transport, and thermoelectric properties of transparent p-type copper iodide thin films. *J. Mater. Chem. C* **11**, 630 (2023).
4. A. Crovetto, H. Hempel, M. Rusu, L. Choubrac, D. Kojda, K. Habicht, T. Unold. Water adsorption enhances electrical conductivity in transparent p-type CuI. *ACS Appl. Mater. Interfaces* **43**, 48741 (2020).
5. A. Liu, H. Zhu, M. Kim, J. Kim, Y. Noh. Engineering copper iodide (CuI) for multifunctional p-type transparent semiconductors and conductors. *Adv. Sci.* **8**, 2100546 (2021).
6. C. Cao, S. Chen, J. Liang, T. Li, Z. Yan, B. Zhang, N. Chen. A high-efficient photo-thermoelectric coupling generator of cuprous iodide. *AIP Advances* **12**, 115125 (2022).
7. O. Caballero-Calero, J. R. Ares, M. Martín-González. Environmentally friendly thermoelectric materials: high performance from inorganic components with low toxicity and abundance in the Earth. *Adv. Sustainable Syst.* **5**, 2100095 (2021).
8. X. Han, Y. Lu, Y. Liu, M. Wu, Y. Li, Z. Wang, K. Cai. CuI/Nylon membrane hybrid film with large Seebeck effect. *Chin. Phys. Lett.* **38**, 126701 (2021).
9. N.P. Klochko, K.S. Klepikova, V.R. Kopach, I.I. Tyukhov, D.O. Zhadan, G.S. Khrypunov, S.I. Petrushenko, S.V. Dukarov, V.M. Lyubov, M.V. Kirichenko, A.L. Khrypunova. Semitransparent p-CuI and n-ZnO thin films prepared by low temperature solution growth for thermoelectric conversion of near-infrared solar light. *Solar Energy* **171**, 704 (2018).
10. N.P. Klochko, K.S. Klepikova, D.O. Zhadan, V.R. Kopach, I.V. Khrypunova, S.I. Petrushenko, S.V. Dukarov, V.M. Lyubov, A.L. Khrypunova. Nanostructured ZnO and CuI thin films on Poly(Ethylene Terephthalate) tapes for UV-shielding applications *J. Nano- Electron. Phys.* **12**, 03007 (2020).
11. S. Koyasu, M. Miyauchi. Recent research trends in point defects in copper iodide semiconductors *J. Electron. Mater.* **49**, 907 (2020).
12. B.R. Sankapal, E. Goncalves, A. Ennaoui, M.Ch. Lux-Steiner. Wide band gap p-type windows by CBD and SILAR methods. *Thin Solid Films* **451–452**, 128 (2004).
13. D.K. Kaushik, M. Selvaraj, S. Ramu, A. Subrahmanyam. Thermal evaporated Copper Iodide (CuI) thin films: A note on the disorder evaluated through the temperature dependent electrical properties. *Solar Energy Materials & Solar Cells* **165**, 52 (2017).
14. M. Dongol, A. El-Denglawey, M.S. Abd El Sadek, I.S. Yahia. Thermal annealing effect on the structural and the optical properties of nano CdTe films. *Optik* **126**, 1352 (2015).
15. D.K. Schroder. *Semiconductor Material and Device Characterization*, 3rd ed. (John Wiley & Sons Inc, 2006) [ISBN: 9780471739067, 0471739065].
16. K.-H. Wu, C.-I. Hung. Effect of substrate on the spatial resolution of Seebeck coefficient measured on thermoelectric films. *Int. J. Therm. Sci.* **49**, 2299 (2010).
17. M. Kneiß, C. Yang, J. Barzola-Quiquia, G. Benndorf, H. von Wenckstern, P. Esquinazi, M. Lorenz, M. Grundmann. Suppression of grain boundary scattering in multifunctional p-type transparent γ-CuI. *Adv. Mater. Interfaces* **5**, 1701411 (2018).
18. N.P. Klochko, K.S. Klepikova, D.O. Zhadan, V.R. Kopach, Y.R. Kostyuchenko, I.V. Khrypunova, V.M. Lyubov, M.V. Kirichenko, A.L. Khrypunova, S.I. Petrushenko, S.V. Dukarov. Transport properties of cubic cuprous iodide films deposited by successive ionic layer adsorption and reaction. In: *Microstructure and Properties of Micro- and Nanoscale Materials, Films, and Coatings (NAP 2019).* Edited by A.D. Pogrebnjak, O. Bondar. *Springer Proceedings in Physics* **240**, (Springer, 2020).
19. P. Sheng. Fluctuation-induced tunneling conduction in disordered materials. *Phys. Rev. B* **21**, 2180 (1980).
20. A. Yildiz, S.B. Lisesivdin, M. Kasap, M. Bosi. Anomalous temperature dependence of the electrical resistivity in In0.17Ga0.83N. *Solid State Commun.* **149,** 337 (2009).
21. X.-L. Shi, J. Zou, Z.-G. Chen. Advanced thermoelectric design: From materials and structures to devices. *Chem. Rev.* **120**, 7399 (2020).
22. Z. Fan, Y. Zhang, L. Pan, J. Ouyang, Q. Zhang. Recent developments in flexible thermoelectrics: From materials to devices. *Renew. Sust. Energ. Rev.* **137**, 110448 (2021).

Received 05.06.2023

Н.П. Клочко, В.Р. Копач,
С.І. Петрушенко, Є.М. Шепотько,
С.В. Дукаров, В.М. Сухов, А.Л. Хрипунова

ЗБАГАЧЕНІ МІДДЮ НАНОСТРУКТУРОВАНІ ПРОВІДНІ ТЕРМОЕЛЕКТРИЧНІ ПЛІВКИ ЙОДИДУ МІДІ(I), ОТРИМАНІ НА ГНУЧКИХ ПІДКЛАДИНКАХ МЕТОДОМ ХІМІЧНОГО ОСАДЖЕННЯ З РОЗЧИНУ

Об'єктами наших досліджень є гнучкі тонкоплівкові термоелектричні матеріали з наноструктурованими шарами CuI товщиною 0,5-1,0 мкм, які виготовлено хімічним осадженням з розчинів методом Послідовної Адсорбції та Реакції Іонних Шарів (SILAR) на гнучких підкладинках з поліетилентерефталату та полііміду. Ці плівки із кубічною структурою γ-CuI відрізняються від отриманих іншими методами хімічного осадження з розчинів, такими як центрифугування, пульверизація та струменевий друк, своїм низьким питомим опором через акцепторні домішки сірки та кисню, які вводяться в CuI з водних розчинів прекурсорів під час осадження SILAR. Енергетичні бар'єри на межах нанозерен CuI розміром 18–22 нм і велика кількість носіїв заряду всередині нанозерен визначають особливості транспорту носіїв заряду в діапазоні температур 295–340 K, які характеризуються переходами від напівпровідникової до металевої поведінки з підвищенням температури, що є характерним для наноструктурованих вироджених напівпровідників. Завдяки питомому опору близько 0,8 мОм $\cdot$ м при 310 K і коефіцієнту Зеєбека 101 мкВ/K, коефіцієнт термоелектричної потужності плівки CuI товщиною 1,0 мкм на поліімідній підкладинці становить 12,3 мкВт/(м $\cdot$ K^2), що відповідає сучасним тонкоплівковим термоелектричним матеріалам p-типу. Це підтверджує придатність отриманих методом SILAR плівок CuI для виготовлення перспективних недорогих нетоксичних гнучких термоелектричних матеріалів.

Ключові слова: купрум(I) йодид, термоелектрика, транспорт носіїв заряду, наноструктура, тонка плівка, процес хімічного осадження з розчинів.